Zhang et al. *NPG Asia Materials* (2025) 17:31
https://doi.org/10.1038/s41427-025-00601-y

NPG Asia Materials

ARTICLE Open Access

Dual dynamic bonds synergy for reusable bio-based adhesive with superior mechanical robustness, environmental reliability, and mildew resistance

Jiayi Zhang[1], Nairong Chen[1], Zhiqiang Zhu[1], Youhui Huang[1], Lihui Chen[1] and Feng Li[1]

Abstract

Introducing dynamics into bio-based adhesives shows many advantages on rendering mechanics and functions. However, the efficient employment of dynamic chemistry in achieving robust, stable, and reusable bio-based adhesives derived from low-value residues remains elusive. Here, we facilely develop a reused camellia meal-based adhesive integrating excellent mechanical robustness, environment durability, and mildew resistance through the cooperation of dual dynamic bonds. By deliberately harnessing dynamic covalent bonds as the first strong interlinking and dynamic noncovalent bonds as the second weak interaction, our strategy allows the resulting adhesive with a much-improved adhesion strength (2.1/1.06 MPa to wood in dry/wet condition) and remarkable adhesion maintenance against harsh environmental factors (organic solvents, salt, acid, alkali, temperature, soaking time). By virtue of these abundant dynamic bonds, this adhesive not only escapes from the inherent drawback of biomaterials to display enlarged anti-mildew efficacy, but also is capable of reprocessing to gain reusability. Combining these desirous characters with the simple two-step fabrication process, this study provides a great potential for the development of high-performance bio-based adhesives sustainably and intelligently.

Introduction

Adhesives are essential for the integration and functionalization of composite materials, showing broad applications in electronics, medicine, construction, labeling, and furnishing[1,2]. Current adhesives are mainly composed of fossil-derived resins[3]. Although the adhesive options are greatly enriched, these fossil-based ones are subjected to reliance of non-renewable resources accompanied with environmental pollution, which pose immense challenges in the green and low-carbon development[1,4]. By contrast, bio-based adhesives, derived from natural biopolymers (such as polysaccharides, proteins, and lignin), have gradually drawn increasing attentions and developed as the promising substitute of fossil-based counterparts, owning to their source renewability, environmental friendliness, and easy availability[5,6]. Nevertheless, pristine bio-based adhesives usually suffer from poor mechanical properties, as mainly imposed by the lack of reliable linkages in biopolymers.

The past few decades have witnessed extensive efforts in improving the mechanical performance of bio-based adhesives by taking advantage of physical modification[7,8], micro/nano-particle strengthening[9,10], or molecular crosslinking[11,12]. Particularly, molecular crosslinking is recognized as the most efficient solution to provide reliable networks, which is commonly driven by static covalent bonds (SCBs)[13]. For example, the covalent crosslinkers containing epoxy or isocyanate groups have widely employed into bio-based adhesives to form permanent molecular linkages, which can remarkably enhance mechanical strength[14,15]. But unfortunately, SCBs also restrict the adhesive network to present rigid and

Correspondence: Nairong Chen (fafucnr@163.com) or Feng Li (lffafu@163.com)
[1]National Forestry and Grassland Administration Key Laboratory of Plant Fiber Functional Materials, College of Materials Engineering, Fujian Agriculture and Forestry University, Fuzhou, China

inadaptable, making them to exhibit considerable limitation in terms of the ever-increasing requirements for the sustainable development of adhesives with reversible and responsive properties[13].

In contrast to the traditional SCBs-driven adhesives, adhesives involving dynamic bonds possess more adaptable networks to response to external stimulus (e.g., force, moisture, or temperature)[16]. Generally, the dynamic bonds can be categorized as dynamic covalent bonds (DCBs) and dynamic noncovalent bonds (DNBs). The former is static at ambient conditions similarly to SCBs, but undergoes reversible dissociation and reformation under stimuli[17–19]. As such, DCBs enable to provide both mechanical robustness and dynamic responsiveness, which usually includes imine bonds[20], disulfide bonds[19], acylhydrazone bonds[21], Diels-Alder reactions[22], and borate ester bonds[18]. And the latter exhibits low association constants that can be easily broken and reformed in response to external stimuli, thereby imparting dynamic properties for the polymer network[23]. DNBs, such as hydrogen bonds, electrostatic associations, π–π complexations, and metal-coordination interactions, have been commonly utilized as sacrificial bonds to enhance the mechanical performance of polymeric adhesives[19,24,25]. To data, dynamic chemistries have been employed to strengthen bio-based adhesives, involving imine bonds, borate ester bonds, multiple hydrogen bonds, and coordination interactions[26,27]. Nevertheless, the previous works mainly focus on elevating the adhesive strength, and are confronted with complicated synthesized method and elaborate molecular regulation. The efficient utilization of dual dynamic bonds synergy on the responsive function of bio-based adhesives, especially for developing the low-value inedible agricultural wastes into high-value functional materials, are still not well understood.

Here, a high-performance bio-based adhesive from inedible agricultural residue is developed by the cooperation of DCBs and DNBs in a two-step method, which is capable of combining reliability and responsiveness together. Such a dual-dynamic-bonds synergy design allows the synthesized adhesive to display robust yet multipurpose adhesion properties (2.1/1.06 MPa to wood in dry/wet condition), and simultaneously presents remarkable endurance to various harsh conditions (organic, salty, acidic, alkaline solutions, extreme temperature, and long-term soaking time). Benefiting from the dynamic chemistry, our adhesive is also demonstrated to function much-improved mildew resistance and reusable efficacy. Distinct from previous bio-based adhesives, our designed adhesive has two significant advantages: (i) inedible agricultural byproduct is utilized to get rid of the issue on food competition; (ii) more excellent functionalities can be successfully integrated via a facile and cost-effective approach. Given these desired adhesive properties and design merits, our strategy endows bio-based adhesive with potential in diverse engineering and intelligent applications, as well as opens new opportunities for the development of agricultural wastes into high-performance functional materials.

Materials and methods

Materials

Camellia meal (CM) containing polysaccharide (41%), protein (16%), tea saponin (14%) and crude fiber (14.7%) was purchased from Tianzhiyuan biotechnology Co., Ltd (Hunan, China). Sodium periodate ($NaIO_4$) and polyethyleneimine (PEI) were purchased from Aladdin Biochemical Technology Co., LTD (Shanghai, China). Poplar veneer with thickness of 1.5 mm were provided by Jiangsu Vidwood Industry Co., Ltd (Jiangsu, China).

Methods

Preparation of OCM/PEI adhesive

The purchased CM was ground into 200 meshes and then mixed in deionized water to form a solution with a solid content of 35%. Then, an appropriate amount of $NaIO_4$ (oxidant) was added into CM solution and then reacted 45 °C in dark environment to oxidize the hydroxyl into aldehyde groups in polysaccharide. After the oxidation of CM, certain weight of PEI was introduced into the OCM solution with 35% solid content to form the resulting OCM/PEI adhesives. For comparison, CM and OCM adhesives were also fabricated.

Characterization

Fourier transform infrared (FTIR) spectra were performed with a Nicolet380 FTIR spectrometer (Thermo Fisher Scientific, Waltham, MA, USA) at a resolution of 4 cm^{-1} and 32 scans. ^1H nuclear magnetic resonance (^1H NMR) spectroscopy were recorded on Bruker 400 M by using TMS as the solvent. Thermal stability of the adhesive was carried out by thermogravimetric analysis (TGA, TA Q600, USA). The samples were heated from 30 to 800 °C at a rate of 10 °C/min at a nitrogen flow rate of 10 mL/min. X-ray photoelectron spectroscopy (XPS) analysis were conducted by using a Thermo Scientific K-Alpha instrument (USA) with Al Kα radiation as the X-ray source. X-ray diffraction (XRD) of the adhesive was analyzed by Rigaku SmartLab SE diffractometer (Rigaku International Corporation, Tokyo, Japan). XRD curves of the adhesive samples were collected from 5° to 90° with a step size of 0.02° under a Cu-Kα source with an acceleration voltage of 40 kV and a current of 40 mA. The surface morphology of adhesive samples was observed by scanning electron microscopy (SEM, Nova Nano SEM 230, USA).

Residual rate measurement

The residual rate was evaluated by using the sol-gel test. The absolutely dry adhesive samples with 40–60 meshes were placed in the condition of 20 ± 1 °C and 70% RH for 24 h. 1 g of adhesive powder was immersed in 100 mL of deionized water at 100 °C for 3 h. The remaining solid residue was then dried at 105 ± 3 °C until the constant mass was achieved. The residual rate was calculated by Eq. (1):

$$\text{Residual rate} = \frac{m_2}{m_1} \times 100\% \quad (1)$$

where m_1 represented the initial mass of the adhesive powder and m_2 was the final mass of dried residue. Each adhesive sample was performed for three times to obtain the average value.

Mechanical properties

The adhesive was applied to poplar veneer surface with a glue content of 225 g/m^2 on each side to form three-layer plywood. And hot-pressing parameters (120 °C, 1 MPa, and 5 min) of glued plywood were determined by the reference of existing bio-based wood adhesives[27–29], ensuring sufficient crosslinking and solidification of adhesive systems[29]. After that, the adhered plywood was stored at 25 °C and 50% RH for 24 h. The adhesion strengths of plywood were carried out based on GB/T17657 –2022. A universal mechanical testing machine (CMT 6104, Shenzhen, China) was used to measure the lap-shear strength of glued plywood at a speed of 10 mm/min. Notably, the dry bonding strength is tested in air condition, and the wet bonding strength was measured by soaking at 63 ± 2 °C water for 3 h and cooled at room temperature for 10 min. The adhesion strengths of OCM/PEI adhesive towards organic, seawater, acidic (pH = 2), alkaline (pH = 13) solutions were evaluated by immersing in the corresponding environment for two days. Also, the adhesion strengths of OCM/PEI adhesive to different soaking temperatures (−80 to 50 °C), varying soaking times (0 to 30 days) in deionized water (25 °C), and other types of substrates (aluminum, copper, glass, and stainless steel) are examined. Prior to the test, these substrates were cleaned with ethanol and deionized water, and then completely dried at room temperature. The adhesive was applied uniformly to the surface of one substrate with an adhesion area of 25 × 25 mm^2 and a glue content of 225 g/m^2 to bond with another one substrate. The following formula used to calculate by the maximum force at failure divided by the overlap area based on five replicates.

Mildew resistance

The mildew resistance measurements of CM, OCM, and OCM/PEI adhesive samples were carried out by placing the samples at a 35 ± 2 °C and 95% RH condition for bacterial incubation. Then, the growth of fungi on the surface of adhesive samples was daily recorded by digital camera.

Reusing adhesion test

The OCM/PEI adhesive was applied to aluminum sheet (size: 80 × 25 × 2 mm^3) with a glue content of 225 g/m^2 and then subjected to hot-pressing (120 °C, 1 MPa) process for 5 min. Subsequently, lap-shear tensile test was carried out to gain the original adhesion strength of OCM/PEI adhesive. The broken adhesive surface was wetted by moisture and then re-bonded under 120 °C and 1 MPa for 5 min. After that, the adhesion strength for the first reprocess was obtained by using lap-shear tensile test. Repeating the same process, the adhesion strength for the second reprocess was achieved.

Results and Discussion

Design and preparation

To construct the dual dynamic bonds network for the bio-based adhesive, we here propose a facile two-step preparation approach. As shown in Fig. 1a, the adhesive is fabricated by employing camellia meal (CM) as biopolymer. CM is an un-edible and low-cost agricultural residue mainly consisting of polysaccharides and proteins[30,31]. Considering the low reactivity of CM, CM is oxidized to transfer hydroxyl (-OH) groups of the polysaccharide into aldehyde (-CHO) and carboxyl (-COOH) groups, thereby acquiring high molecular reactivity. Then, polyethyleneimine (PEI) with abundant amine groups (-NH_2) is imported into oxidized CM (OCM) to provide dynamic interacting sites for adhesive network. In the designed OCM/PEI adhesive, imine bonds are generated through the Schiff base reaction between OCM and PEI, which is acted as DCBs for the first strong linkages, and also, noncovalent linkages (hydrogen bonds and ionic bonds) are existed as DNBs for the second weak associations (Fig. 1b). The fabricated adhesive is revealed to exhibit strong bonding behavior to diverse substrates, including wood, ceramic, Teflon, glass, rubber, and steel (Fig. 1c). As uncovered by Fig. 1d, such an improved adhesiveness of OCM/PEI adhesive is mainly attributed by its more compact and adaptable structure than those of CM and OCM adhesives. Thus, the dual dynamic bonds network working cooperatively is speculated to impart the OCM/PEI adhesive with reliability and responsiveness together.

Structural characterization and proposed mechanism

We then analyze the structure of OCM/PEI adhesive by taking advantage of a series of characterization. FTIR spectra (Fig. 2a, b) reveal that, compared to pure CM, OCM exhibits the decreased intensity of υ (-OH) peak at 3323 cm^{-1} and the disappearance of δ (-OH) peak at

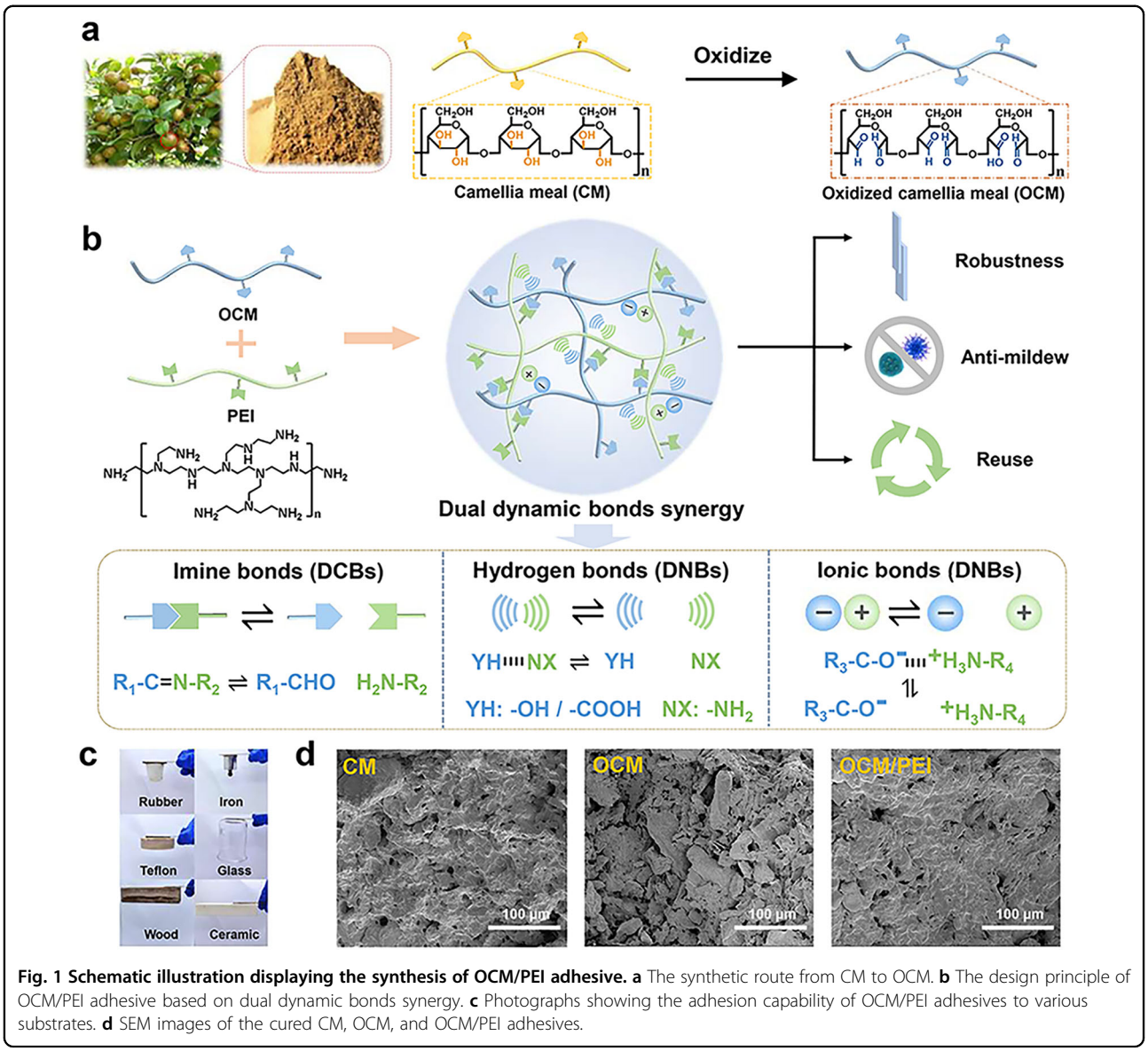

Fig. 1 Schematic illustration displaying the synthesis of OCM/PEI adhesive. a The synthetic route from CM to OCM. **b** The design principle of OCM/PEI adhesive based on dual dynamic bonds synergy. **c** Photographs showing the adhesion capability of OCM/PEI adhesives to various substrates. **d** SEM images of the cured CM, OCM, and OCM/PEI adhesives.

1655 cm^{-1}, which could be attirbuted to the oxidation of −OH groups into −CHO groups[32,33]. In addition, υ (−C = O) peak shifts from 1738 to 1735 cm^{-1} after oxidation, further demonstrating the successful oxidation of CM[33]. While the lower υ (−C = O) peak intensity in OCM may be due to the partial consumption of aldehyde groups through the Schiff base reaction between with aldehyde groups of OCM and amine groups of protein component existed in CM[32]. After combining PEI with OCM, OCM/PEI adhesive can form imine bonds between −CHO groups in OCM and $–NH_2$ groups in PEI, as evidenced by the appearance of −C = N peak (1660 cm^{-1})[34,35]. The amidation reaction is also observed in OCM/PEI adhesive, as supported by the shift of −C-N peak (1249 → 1263 cm^{-1}) and the decreased intensity of −OH peak derived from carboxyl groups (1421 cm^{-1})[36,37]. Besides, the existence of hydrogen bonds and electrostatic interactions in OCM/PEI adhesive is demonstrated by the shift of υ (-OH/-N-H) peak from 3377 to 3350 cm^{-1} presented in Fig. 2 and the charge neutralization observed in Figure S1a, respectively. The imine bonds formed in OCM/PEI adhesive can be further testified by XPS measurements. As displayed in Fig. 2c, the O 1 s curve of CM adhesive can be fitted into three peaks, including C-O-C, −C−OH, and −C = O peaks, which are assigned to the glycosidic bond of polysaccharides, the C-O stretching vibrations from hydroxyl groups of polysaccharides, and the carbonyl groups of OCM, respectively[32,34]. OCM adhesive exhibits an enhanced intensity of −C = O peak (531.7 eV), indicating the formation of more −CHO groups in OCM. For OCM/PEI adhesive, XPS curves presented in Fig. 2c, d exhibit a

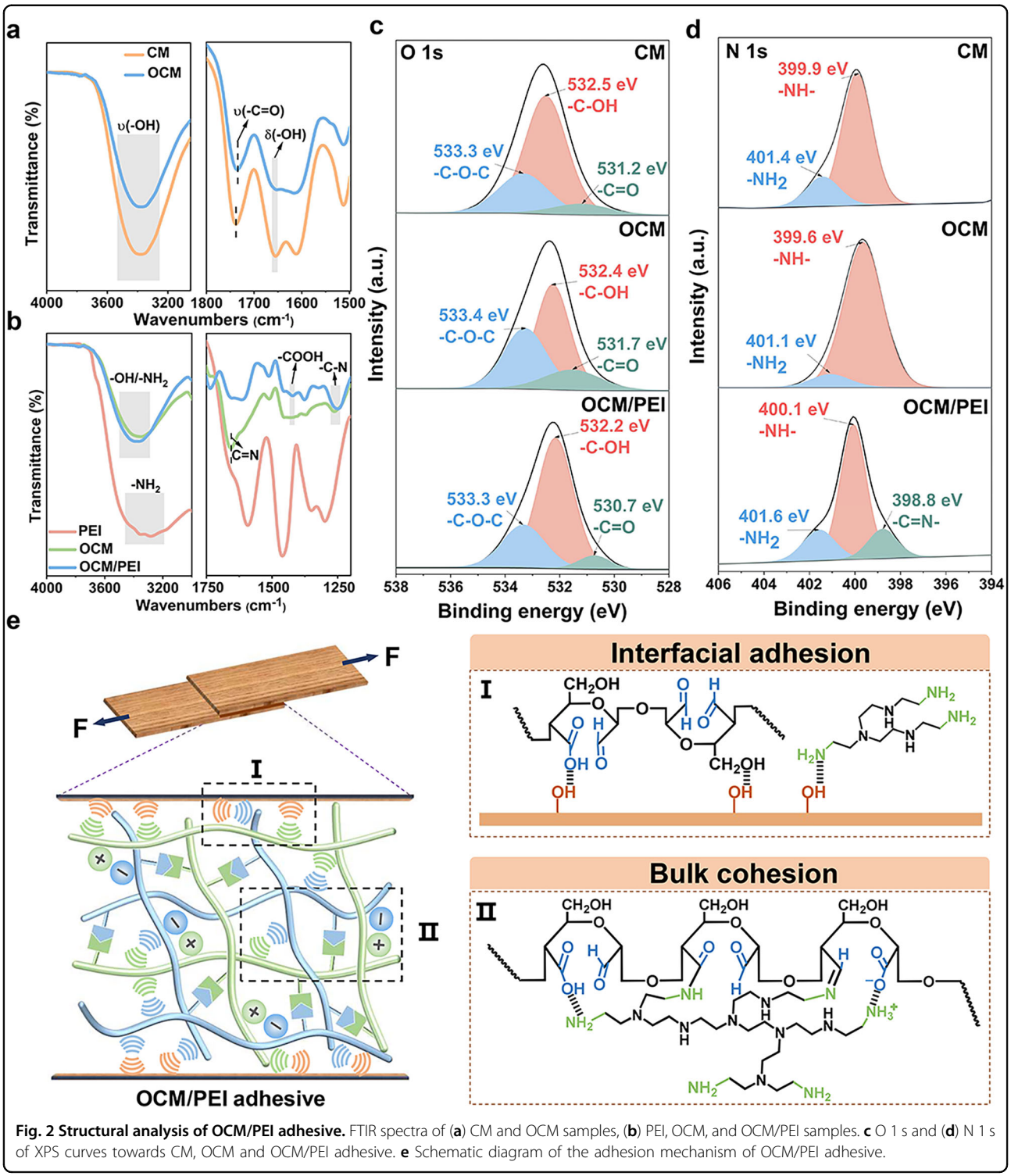

Fig. 2 Structural analysis of OCM/PEI adhesive. FTIR spectra of (**a**) CM and OCM samples, (**b**) PEI, OCM, and OCM/PEI samples. **c** O 1 s and (**d**) N 1 s of XPS curves towards CM, OCM and OCM/PEI adhesive. **e** Schematic diagram of the adhesion mechanism of OCM/PEI adhesive.

decrease of −C = O peak and a appearance of new –N= peak (399.3 eV), suggesting the successful aldehyde-amine crosslinks between OCM and PEI molecules[32,38]. Notably, OCM adhesive presents a weakened $–NH_2$ peak compared to CM adhesive, which might ascribe to the crosslink of −CHO groups with the $–NH_2$ groups of proteins existed in CM.

XRD analysis also carries out to assess the structural stability of OCM/PEI adhesive. As shown in Figure S1b, compared with CM, OCM exhibits the weakened

crystallization peaks (9.0° and 20.1°) with a decreased crystallinity, implying that the oxidation process can partially destroy the crystallization structure of CM molecules[32,33]. The import of PEI enables the adhesive crystallinity to largely increase, mainly as a result of the abundant DCBs and DNBs formed between OCM and PEI. The stability of OCM/PEI adhesive is further supported by TG curves, showing the highest weight residue and lowest degradation rate (Figure S1c, d). Remarkably, the maximum degradation temperature of OCM/PEI adhesive decreases to 307 °C, which is mainly attributed to the introduction of abundant dynamic bonds and thereby imparts the higher dynamic capability under stimuli of heating. Taken together, the coexistence of DCBs (imine bonds) and DCBs (hydrogen bonds and electrostatic interactions) leads to an adaptable crosslinking network of OCM/PEI adhesive, which theoretically contributes to the robust bulk cohesion in adhesive and the strong interfacial adhesion with substrates (Fig. 2e).

Adhesion properties

To gain insight into the effect of dual dynamic network on adhesion properties, we first synthesize a family of OCM/PEI adhesives by varying oxidant ratio and oxidation time of OCM. As presented by Fig. 3a and Figure S2a, the higher dry/wet adhesion strength of OCM/PEI adhesive is obtained with the more oxidant contents, which reaches the maximum (2.4/1.06 MPa) when the oxidant ratio is 7.7 wt% (relative to CM). This ascribes to that the more oxidants contribute to the higher oxidized degree of CM, thereby imparting more active –CHO/-COOH groups to form DCBs (namely, imine/amide bonds) with PEI. Note that CM/PEI adhesive without oxidation displays wet adhesion failure, further reflecting the unstable interactions between CM and PEI molecules. When the oxidant content is above 7.7 wt%, the adhesion strength turns to decrease, because that the excessive oxidants may lead to the over-degradation of CM molecules. In addition to oxidant content, oxidation time also affects the adhesion property of OCM/PEI adhesive (Fig. 3b and Figure S2b). By gradually extending oxidation time to 20 h, OCM/PEI adhesive shows the enhanced dry/wet adhesion strength. This observation is mainly attributed to that the longer oxidation time results in the higher oxidized degree of CM, thus enabling more DCBs between OCM and PEI. Further prolonging oxidation time to 24 h causes the declined adhesion efficacy, the reason of which is similar to that of the over-high oxidant contents.

We then study the adhesion properties of OCM/PEI adhesive by changing PEI with different molecular weights and addition quantities. In Fig. 3c and Figure S2c, as increasing molecular weight of PEI to 10,000, despite the reactivity of PEI is affected, both dry and wet adhesion strength of OCM/PEI adhesive improve. It is not only attributed to the enhanced mechanical strength of PEI molecule, but also may ascribe to that the hot-pressing process contributes to sufficient covalent crosslinks between OCM and PEI[29]. When the molecular weight of PEI is above 10,000, the dry adhesion strength of OCM/PEI adhesive further increase while the wet adhesion strength turns to decrease. This finding is probably attributed to that the continuously deceased reactivity of PEI makes it failing to react with OCM even at hot-pressing process, thus leading to less strong DCBs and more DNBs formed in OCM/PEI adhesive[39,40]. Both DCBs and DNBs contribute to the resultant dry adhesion strength, but for wet condition, DNBs are easily broken by water and thus causes the weakened strength[31]. In addition, as increasing PEI content to 5% (related to CM), OCM/PEI adhesive shows a gradually elevated adhesion strength (Fig. 3d and Figure S2d). This is attributed to the formation of more imine bonds via Schiff base reaction, as evidenced by the stronger C = N peak intensity in Figure S1e. While the PEI content is above 5%, the adhesion strength appears to decrease, mainly ascribing to two underlying reasons: (1) over-high content of PEI (> 5%) endows OCM/PEI adhesives with much-enhanced flexibility, which leads to the less stiffness and thus the decreased mechanical strength[41]; (2) higher content of PEI contains more unreacted hydrophilic amine groups, resulting in the instability of adhesive network and thus the decreased adhesion strength. These above findings have successfully manifested that the mechanical performance of OCM/PEI adhesive can easily be tailored and improved by virtue of the synergistic dual dynamic bonds. Further, we compare the mechanical performances between CM/PEI adhesive connected by NCBs and OCM/PEI adhesive consisting of DCBs and NCBs. As presented in Figure S3, OCM/PEI adhesive exhibits higher adhesion strength than CM/PEI one, powerfully demonstrating the synergistic effect of DCBs and NCBs on improving adhesion performance.

To further evaluate the practicability of OCM/PEI adhesive, we measure its endurance towards various harsh environments. Figure 3e reveals that OCM/PEI adhesive can sustain high adhesion strength after submerging in diverse aqueous conditions, including N, N-dimethylformamide (DMF), acetonitrile, dichloromethane (DCM), ethanol, seawater, acidic (pH = 2), and alkaline (pH = 13) solutions for two days. The high stability of OCM/PEI adhesive to various solutions could be attributed to the formed interpenetrating polymer network between high-molecule-weight OCM and PEI. Such a network can prevent ion penetration from disrupting hydrogen bonds[42,43]. The effect of temperature and soaking time on wet adhesion strength are also investigated. As shown in Fig. 3f and Figure S4, OCM/PEI adhesive not only shows excellent water resistance over a

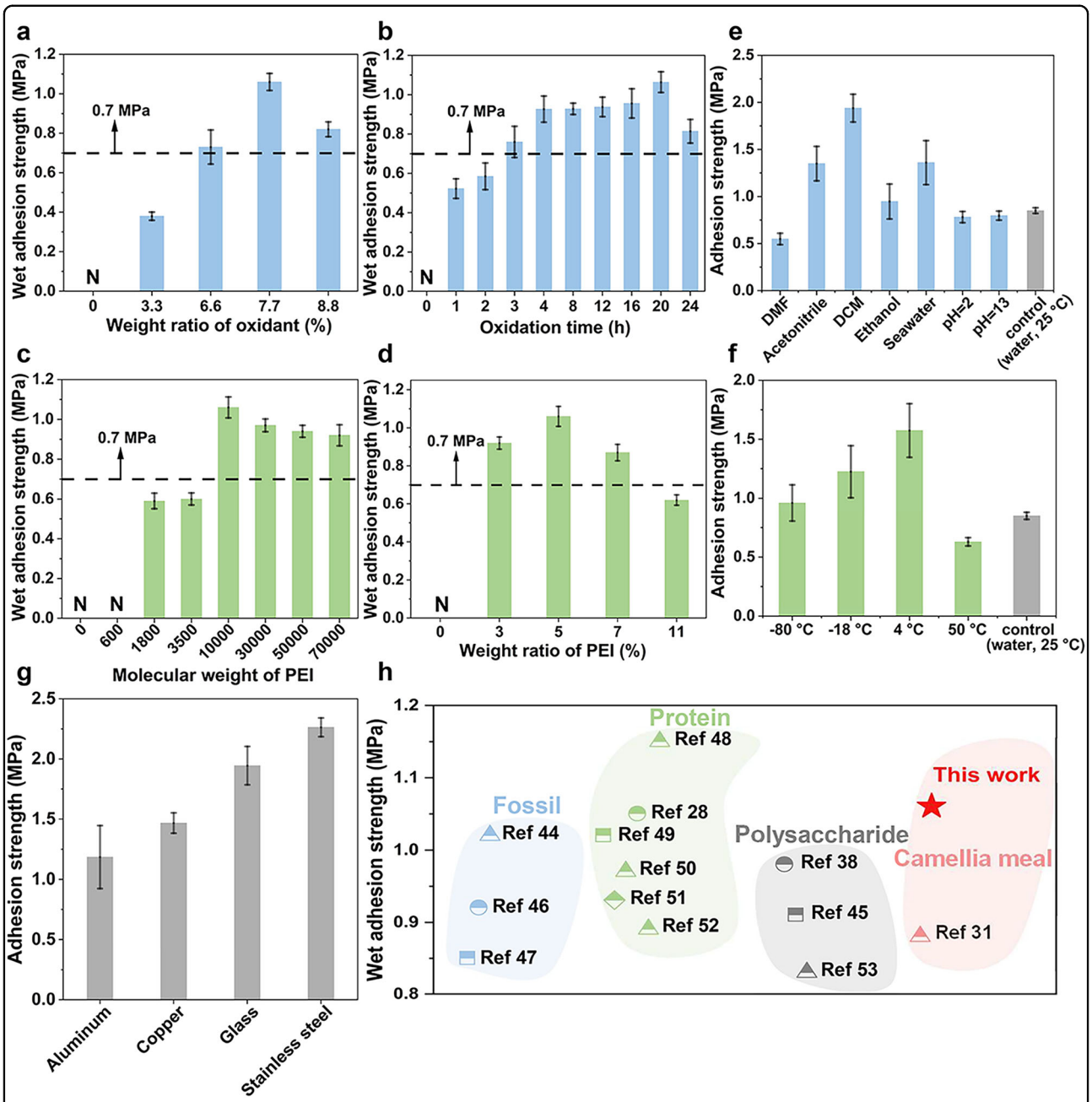

Fig. 3 Adhesion measurement of OCM/PEI adhesive. The wet adhesion strength of OCM/PEI adhesives with different (**a**) weight ratio of oxidant (relative to CM), (**b**) oxidation time, (**c**) molecular weight and (**d**) weight ratio of PEI (relative to CM). The wet adhesion strength of OCM/PEI adhesives (**e**) under varied submerged solutions, (**f**) in water with various temperatures, and (**g**) to different substrates. **h** The adhesion comparison of OCM/PEI adhesives with the other literature-reported adhesive systems.

wide temperature range from −80 °C to 50 °C, but also maintains high adhesion strength even after immersing in water for 30 days. This superior stability presented in OCM/PEI adhesive may ascribe to the synergy of DCBs and NCBs that is of benefit to better adaptability towards various harsh environments, which is further evidenced by the higher residue rate and water contact angle compared to CM and OCM adhesives (Figure S1f). Furthermore, OCM/PEI adhesive is uncovered to be capable of strongly bonding diverse substrates (including aluminum, copper, glass, and stainless steel), manifesting its multipurpose adhesion behavior (Fig. 3g). As depicted in Fig. 3h, the adhesion superiority of OCM/PEI adhesive is successfully demonstrated by comparison with the

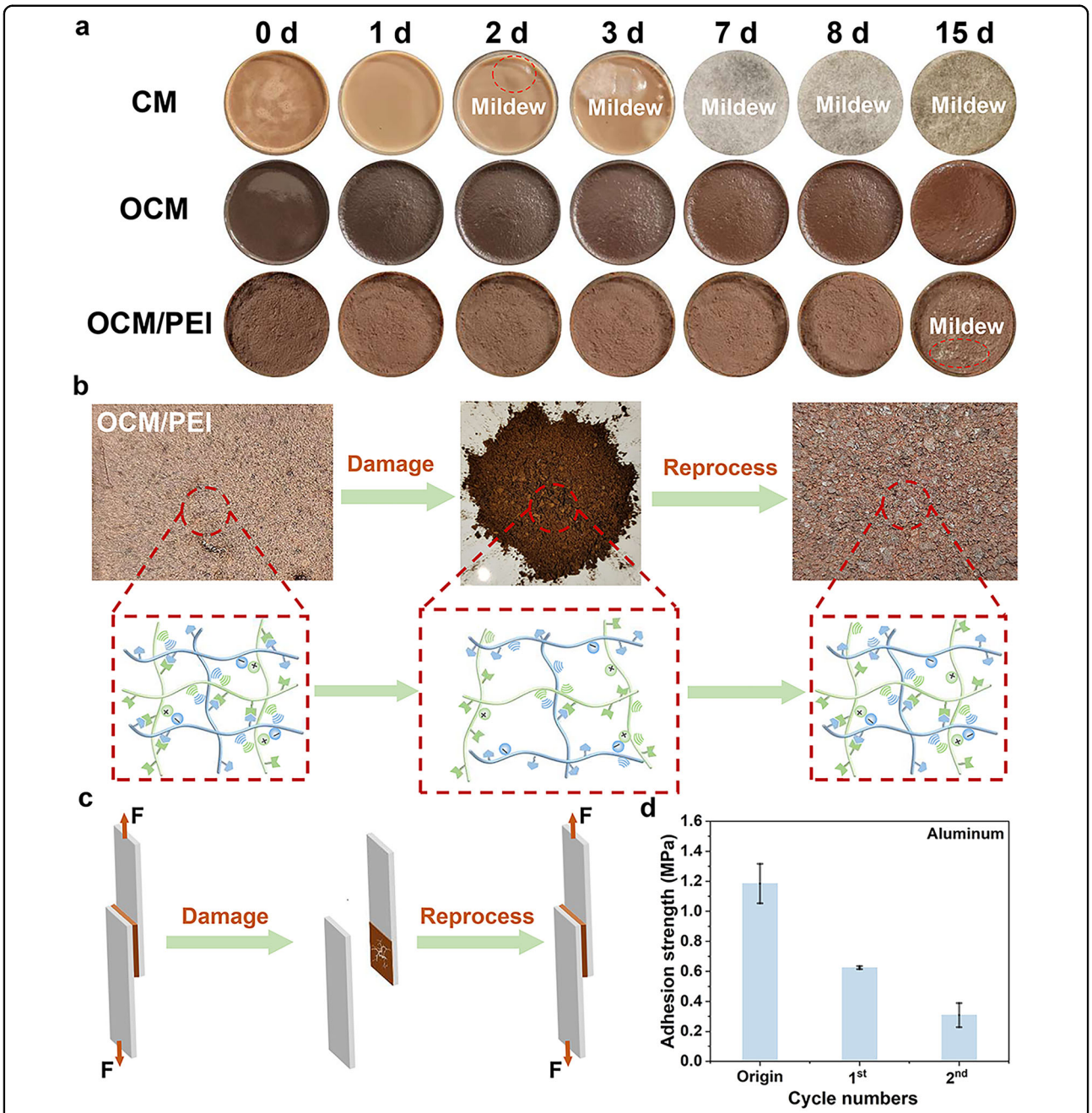

Fig. 4 Application assessment of OCM/PEI adhesive. a Mildew resistance test of CM, OCM, and OCM/PEI adhesives. **b** The optical images and the rearrangement mechanism of OCM/PEI adhesive samples. **c** Schematic diagram of reprocessing process and (**d**) the adhesion strength of OCM/PEI adhesives to aluminum substrates under three cycle numbers.

existing fossil-derived and bio-based adhesives reported by literatures[28,31,38,44–53].

Anti-mildew and reusable performances

Mildew resistance is of great importance to the adhesive properties, especially for the bio-derived adhesives[53]. As shown in Fig. 4a, pristine CM adhesive is prone to mould and appears to moldy within 3 days. The oxidation modification enables OCM adhesive without mildew even after storing at 30 ± 2 °C and 90% RH condition for 15 days, probably because the its abundant aldehyde groups that can react with protein of bacteria and thereby inhibit their growth[54]. However, despite the remarkable anti-mildew property, OCM adhesive is unpractical due to its unsatisfied adhesion strength. For the high-strength OCM/PEI adhesive, the anti-mildew efficacy has

improved along with the gradually raising PEI content, as reflected by the extended anti-mildew time from 3 to 15 days (Fig. 4a and Figure S5). Such an excellent mildew resistance mainly benefits from two factors: one is the cationic amino groups existed in PEI, and the other is the aldehyde groups derived from OCM, both of which cooperate to effectively kill mildew via electrostastic interactions between OCM/PEI adhesive and mildew protein[55]. Notably, compared to OCM adhesive, OCM/PEI sample exhibits decreased mildew resistance. This may be attributed to the consume of free amine and aldehyde groups via Schiff base reaction between OCM and PEI, leading to the weakened anti-mildew effect[32]. Though OCM/PEI-4 adhesive degraded after 15 days, it is much-improved compared to CM adhesive (degraded within 2 days). Such a character can satisfy the application requirements of bio-based adhesives[56,57]. Additionally, when OCM/PEI adhesive cured, the formed imine bonds between OCM and PEI can further enhance structural stability, which can be reflected by the superior long-term durability towards underwater conditions shown in OCM/PEI adhesive (Figure S4, maintaining high adhesion even after soaking 30 days). Thus, OCM/PEI adhesive is capable of presenting long-term stability towards humid environment during actual application.

Owning to the dynamic covalent-noncovalent bonds synergy, OCM/PEI adhesive is also expected to exhibit reusable adhesion behavior. As observed in Fig. 4b, the cured OCM/PEI adhesive sample is damaged into pieces to present a disconnected molecule network. Interestingly, the broken structure of OCM/PEI adhesive can rearrange and reform under the stimuli of moisture and hot pressing (120 °C, 1 MPa), as reflected by the successful jointing of pieces into a compact bulk. To further assess the reusability of OCM/PEI adhesive, we then measure its lap-shear adhesion strength via cyclic bonding and debonding test (Fig. 4c). As shown in Fig. 4d, the adhesion strength can restore to 53% of the original for the first cycle and 26% of the original for the second cycle, which suggests that dynamic bonds were reformed between OCM and PEI, including DCBs (imine bonds) and DNBs (hydrogen bonds and electrostatic interactions). The partial mechanical loss probably results from the formation of stable imine bonds and the unoxidized biopolymers featuring nondynamic nature in CM (such as protein), which restricts the reversibility and mobility of OCM/PEI adhesive network.

Conclusion

In summary, we engineer a unique CM-based adhesive by the dual dynamic bonds synergy, which rationaly leverages DCBs as first reliable linkages and DNBs as the second weak assications. As such, the adhesive is demonstrated to possess remarkable adhesion performance that can strongly bond to diverse sbustrates, as well as resist to various harsh sumberged enviroments. The synergistc effect of DCBs and DNBs also enables the adhesive with much-improved mildew resistance and reusability. This work provides a feasible way for the sustainable and intellengent development of bio-based adhesives with superior comprehensive performance.

Acknowledgements
The authors acknowledge the support from the National Natural Science Foundation of China (No. 32371795 and No. 31971592), the District Development Project of Fujian province (No. 2022Y3006), the Project of young teacher education research of Fujian province (No. JZ230016), the Project of Fujian province (No. 2024J01404) and the Innovation fund program of Fujian Agriculture and Forestry University, China (No KFB24002A and KFB24004A).

Author contributions
Z.J. and L.F. conceived the concept of this work. Z.J. carried out all the experiments with the assistance of Z.Z., H.Y., C.L. and L.F. Z.J. took primary responsibility for writing, while L.F. and C.N. advised on the overall structure of the manuscript and revised the manuscript. All authors jointly analyzed the data and provided useful discussions and commented on the manuscript.

Data availability
All data are available in the manuscript or the supplement materials. Information requests should be directed to the corresponding author.

Conflict of interest
The authors declare no competing interests.

Ethics approval and consent to participate
This study does not involve human participants, animal subjects, or sensitive personal data. All experiments and analyses were conducted using publicly available data/materials or in compliance with standard laboratory protocols.

Publisher's note
Springer Nature remains neutral with regard to jurisdictional claims in published maps and institutional affiliations.

Supplementary information The online version contains supplementary material available at https://doi.org/10.1038/s41427-025-00601-y.

Received: 17 August 2024 Revised: 19 March 2025 Accepted: 3 April 2025.
Published online: 8 August 2025

References

1. Westerman, C. R., McGill, B. C. & Wilker, J. J. Sustainably sourced components to generate high-strength adhesives. *Nature* **621**, 306–311 (2023).
2. Cui, C. & Liu, W. Recent advances in wet adhesives: Adhesion mechanism, design principle and applications. *Prog. Polym. Sci.* **116**, 101388 (2021).
3. Yang, G., Gong, Z., Luo, X., Chen, L. & Shuai, L. Bonding wood with uncondensed lignins as adhesives. *Nature* **621**, 511–515 (2023).
4. Li, M., Mao, A., Guan, Q. & Saiz, E. Nature-inspired adhesive systems. *Chem. Soc. Rev.* **53**, 8240–8305 (2024).
5. Zuiderveen, E. A. R. et al. The potential of emerging bio-based products to reduce environmental impacts. *Nat. Commun.* **14**, 8521 (2023).
6. Arias, A. et al. Recent developments in bio-based adhesives from renewable natural resources. *J. Clean. Prod.* **314**, 127892 (2021).
7. Pi, B. S. et al. Processable, reversible, and reusable 100% bio-based pressure sensitive adhesives using nanostarch. *Chem. Eng. J.* **495**, 153392 (2024).
8. Sun, X. et al. All-cellulose hydrogel-based adhesive. *Innov. Mater.* **1**, 100040 (2023).
9. Subagia, I. A. et al. Mechanical performance of multiscale basalt fiber–epoxy laminates containing tourmaline micro/nano particles. *Compos. Part B. Eng.* **58**, 611–617 (2014).

10. He, X. et al. Ultrastretchable, Adhesive, and Antibacterial Hydrogel with Robust Spinnability for Manufacturing Strong Hydrogel Micro/Nanofibers. *Small* **17**, 2103521 (2021).
11. Sun, P., Qin, B., Xu, J.-F. & Zhang, X. High-Performance Supramolecular Adhesives. *Macromol. Chem. Phys.* **224**, 2200332 (2023).
12. Jiang, S. et al. Long-Chain Polyamine-Glyoxal Wood Adhesive: Formaldehyde-Free, Green Synthesis, and Ultra-Performances. *ACS Sustain. Chem. Eng.* **11**, 13209–13221 (2023).
13. Chen, M. et al. Fast, strong, and reversible adhesives with dynamic covalent bonds for potential use in wound dressing. *Proc. Natl Acad. Sci. USA* **119**, e2203074119 (2022).
14. Guo, X. et al. Bioinspired Injectable Polyurethane Underwater Adhesive with Fast Bonding and Hemostatic Properties. *Adv. Sci.* **11**, 2308538 (2024).
15. Farzanehfar, N., Taheri, A., Rafiemanzelat, F. & Jazani, O. M. High-performance epoxy nanocomposite adhesives with enhanced mechanical, thermal and adhesion properties based on new nanoscale ionic materials. *Chem. Eng. J.* **471**, 144428 (2023).
16. Zhao, X.-L., Tian, P.-X., Li, Y.-D. & Zeng, J.-B. Biobased covalent adaptable networks: towards better sustainability of thermosets. *Green. Chem.* **24**, 4363–4387 (2022).
17. Webber, M. J. & Tibbitt, M. W. Dynamic and reconfigurable materials from reversible network interactions. *Nat. Rev. Mater.* **7**, 541–556 (2022).
18. Chakma, P. & Konkolewicz, D. Dynamic covalent bonds in polymeric materials. *Angew. Chem. Int. Ed.* **58**, 9682–9695 (2019).
19. Zhao, J., Zhang, Z., Wang, C. & Yan, X. Synergistic dual dynamic bonds in covalent adaptable networks. *CCS Chem.* **6**, 41–56 (2024).
20. Li, Z. et al. Integration of Aromatic Polyurea and Dialdehyde Cellulose as High-Performance Hybrid Resin Adhesives for Bonding Wood. *ACS Sustain. Chem. Eng.* **11**, 11878–11889 (2023).
21. Wang, L. et al. Multifunctional polymer composite coatings and adhesives by incorporating cellulose nanomaterials. *Matter* **6**, 344–372 (2023).
22. Luo, T. et al. Fabrication of well-defined lignin-derived elastomers by atom transfer radical polymerization and Diels-Alder reaction towards sustainable, super-tough and high temperature-resistant hot-melt adhesives. *Chem. Eng. J.* **479**, 147729 (2024).
23. Davoud, M. & Zhibin, G. Enhancing Mechanical Performance of a Covalent Self-Healing Material by Sacrificial Noncovalent Bonds. *J. Am. Chem. Soc.* **137**, 4846–4850 (2015).
24. Zhang, J. et al. Small-molecule ionic liquid-based adhesive with strong room-temperature adhesion promoted by electrostatic interaction. *Nat. Commun.* **13**, 5214 (2022).
25. Rodin, M., Li, J. & Kuckling, D. Dually cross-linked single networks: structures and applications. *Chem. Soc. Rev.* **50**, 8147–8177 (2021).
26. Zeng, G. et al. Desirable Strong and Tough Adhesive Inspired by Dragonfly Wings and Plant Cell Walls. *ACS Nano* **18**, 9451–9469 (2024).
27. Zhou, Y. et al. Design of tough, strong and recyclable plant protein-based adhesive via dynamic covalent crosslinking chemistry. *Chem. Eng. J.* **460**, 141774 (2023).
28. Yang, H. et al. Development of biomass adhesives based on aminated cellulose and oxidized sucrose reinforced with epoxy functionalized wood interface. *Compos. Part B Eng.* **263**, 110872 (2023).
29. Yin, C. et al. Developing a water-resistant cellulose-based wood adhesive based on dual dynamic Schiff base and disulfide bonds. *Ind. Crops Prod.* **209**, 118011 (2024).
30. Ma, Y. et al. Research advances in bio-based adhesives. *Int. J. Adhes. Adhes.* **126**, 103444 (2023).
31. Wang, H., Zhao, S., Zhang, W., Zhang, S. & Han, Y. Camellia meal-based adhesive with synergistic crosslinking of physical and chemical interaction for preparing aldehyde-free, anti-mildew, water-resistant wood-based composites. *J. Clean. Prod.* **451**, 142091 (2024).
32. Wang, H. et al. Camellia meal-based formaldehyde-free adhesive with self-crosslinking, and anti-mildew performance. *Ind. Crops Prod.* **176**, 114280 (2022).
33. Pozo, C. et al. Study of the structural order of native starch granules using combined FTIR and XRD analysis. *J. Polym. Res.* **25**, 1–8 (2018).
34. Li, J. et al. Multi-scale structure characterization of ozone oxidized waxy rice starch. *Carbohydr. Polym.* **307**, 120624 (2023).
35. Mees, M. A., McAllister, T. D., Curia, S., Howdle, S. M. & Hoogenboom, R. Modification of linear polyethylenimine with supercritical CO2: From fluorescent materials to covalent cross-links. *Macromolecules* **56**, 2841–2851 (2023).
36. Guo, Q. et al. Hydrogen-bonds mediate liquid-liquid phase separation of mussel derived adhesive peptides. *Nat. Commun.* **13**, 5771 (2022).
37. Shi, Y., Wu, B., Sun, S. & Wu, P. Aqueous spinning of robust, self-healable, and crack-resistant hydrogel microfibers enabled by hydrogen bond nanoconfinement. *Nat. Commun.* **14**, 1370 (2023).
38. Song, J. et al. Developing on the well performance and eco-friendly sucrose-based wood adhesive. *Ind. Crops Prod.* **194**, 116298 (2023).
39. Zeng, G. et al. A bio-based adhesive reinforced with functionalized nanomaterials to build multiple strong and weak cross-linked networks with high strength and excellent mold resistance. *Chem. Eng. J.* **453**, 139761 (2023).
40. Al-Absi, A. A., Ogungbenro, A. E., Benneker, A. M. & Mahinpey, N. Review of polyethylenimine through ring-opening polymerization reactions and its application in CO_2 capture. *J. Environ. Chem. Eng.* **12**, 112739 (2024).
41. Xu, F., Park, H. E. & Cho, B.-U. Porous carboxymethylcellulose/polyethyleneimine composite beads: formation process, enhanced physical properties, and pH-induced response mechanism. *Cellulose* **31**, 6295–6316 (2024).
42. Zhao, T. et al. A high-adhesive and sensitive hydrogel with interpenetrating and interlocking networked structure for efficient biological signal monitoring. *Polymer* **304**, 127121 (2024).
43. Xu, C. et al. Mechanical Regulation of Polymer Gels. *Chem. Rev.* **124**, 10435–10508 (2024).
44. Peng, J. et al. Characterization on the Copolymerization Resin between Bayberry (Myrica rubra) Tannin and Pre-Polymers of Conventional Urea–Formaldehyde Resin. *Forests* **13**, 624 (2022).
45. Cao, L. et al. Preparation and characterization of a novel environment-friendly urea-glyoxal resin of improved bonding performance. *Eur. Polym. J.* **162**, 110915 (2022).
46. Zhang, Q. et al. Preparation of Environmentally Friendly Urea-Hexanediamine-Glyoxal (HUG) Resin Wood Adhesive. *J. Renew. Mater.* **12**, 235–244 (2024).
47. Pang, B. et al. The direct transformation of bioethanol fermentation residues for production of high-quality resins. *Green. Chem.* **22**, 439–447 (2020).
48. Liu, X. et al. Hybrid HNTs-kenaf fiber modified soybean meal-based adhesive with PTGE for synergistic reinforcement of wet bonding strength and toughness. *Int. J. Adhes. Adhes.* **87**, 173–180 (2018).
49. Zhang, J. et al. An easy-coating, versatile, and strong soy flour adhesive via a biomineralized structure combined with a biomimetic brush-like polymer. *Chem. Eng. J.* **450**, 138387 (2022).
50. Jiang, K. et al. Improved performance of soy protein adhesive with melamine–urea–formaldehyde prepolymer. *RSC Adv.* **11**, 27126–27134 (2021).
51. Li, H., Kang, H., Zhang, W., Zhang, S. & Li, J. Physicochemical properties of modified soybean-flour adhesives enhanced by carboxylated styrene-butadiene rubber latex. *Int. J. Adhes. Adhes.* **66**, 59–64 (2016).
52. Luo, J., Zhou, Y., Gao, Q., Li, J. & Yan, N. From Wastes to Functions: A New Soybean Meal and Bark-Based Adhesive. *ACS Sustain. Chem. Eng.* **8**, 10767–10773 (2020).
53. Zeng, H. et al. Boiling water resistant fully bio-based adhesive made from maleated chitosan and glucose with excellent performance. *Int. J. Biol. Macromol.* **253**, 127446 (2023).
54. Xu, C. et al. Soy protein adhesive with bio-based epoxidized daidzein for high strength and mildew resistance. *Chem. Eng. J.* **390**, 124622 (2020).
55. Zhou, Y. et al. Tough, Waterproofing, and Sustainable Bio-Adhesive Inspired by the Dragonfly Wing. *Adv. Funct. Mater.* **34**, 2406557 (2024).
56. Zhang, J. et al. Dual-crosslinked ascidian larvae-inspired strong soy flour adhesive with excellent coating, prepressing adhesion and mildew-resistance performance. *Ind. Crops Prod.* **220**, 119270 (2024).
57. Zhu, Z. et al. A robust, storable, and controllable cold-set protein adhesive enabled by Pickering emulsion-templated microcapsules. *Cell Rep. Phys. Sci.* **5**, 102266 (2024).